Inelastic neutron scattering from solid krypton at 10 °K*

J. Skalyo, Jr., Y. Endoh,† and G. Shirane
Brookhaven National Laboratory, Upton, New York 11973
(Received 23 August 1973)

The phonon dispersion of fcc krypton has been measured along high-symmetry directions at 10 °K on a single crystal with an equilibrium lattice spacing of 5.646 ± 0.002 A. The data can be fitted with a general three-neighbor-force-constant model of nine parameters with only slight depatures from central force axially symmetric conditions. Utilizing theoretical estimates of the weak additional forces due to the fourth- through eighth-nearest neighbors, the zero-sound elastic constants are determined to be $c_{11} = 514 \pm 5$, $c_{12} = 284 \pm 6$, and $c_{44} = 268 \pm 3 \times 10^8$ dyn cm^{-2}. The agreement of the measured dispersion curves with theoretical calculations by Barker *et al.* is excellent; the maximum deviation of $\approx 3\%$ occurs near the zone boundary. A broadening of the neutron response for zone-boundary modes was observed that was comparable to the energy itself when the sample was near its melting point.

I. INTRODUCTION

The heavy-rare-gas elements provide ideal substances for the comparison of theoretical and experimental phonon dispersion throughout their solid range of temperatures. As the Debye temperatures of the rare solids are about the same (save for helium), the higher melting temperatures of the heavier species permit a wider range of anharmonicity to be studied. In the case of helium, the lattice dynamics are dominated by effects arising from large zero-point motion. Alternatively, in regard to the present study, the heavy mass of the krypton atom minimizes the effects of zero-point motion; hence consideration of the theoretical complications of hard-core correlations and the application of self-consistent phonon theory are not mandatory in obtaining theoretical estimates for comparison with experiments performed at liquid-helium temperatures. In particular, it is of interest to measure the deviation from the Cauchy relation $\delta = (c_{44} - c_{12})/c_{12}$. The difference can be an indication of the strength of three-body forces, since $c_{44} = c_{12}$ for two-body central forces and no zero-point motion.

The first dispersion measurement in single crystals of rare-gas solids was done by Daniels *et al.*[1] on krypton at 79 °K. These authors used an aluminum-alloy pressure cell to grow the crystal; the melting line was crossed at 166 °K and 2.31 kbar. Measurements were made in several symmetry directions after a near-isochoric reduction in temperature gave a lattice constant of 5.725 ± 0.010 Å at approximately 0.3 kbar. Their study showed the forces to be predominantly near neighbor and of central character. The high-pressure method is suitable in preserving the integrity of the sample only so long as a positive pressure can be sustained. A crystal stable at the 0 °K lattice spacing could therefore be grown and offer a substantial range over which the anharmonic temperature effects could be studied; the near-isochoric state of the sample effectively removes the otherwise more prominent volume dependence of the dispersion. Just such a technique has already been utilized in investigations of the temperature dependence of the dispersion in neon by Leake *et al.*[2] and by Skalyo *et al.*[3] where the melting line was crossed at 0.7 kbar and 35 °K to give samples with the zero-pressure lattice constant at 5 °K. A much wider temperature range for investigation is possible with the heavier-rare-gas solids. The density of solid argon on the melting line has been measured by Crawford and Daniels[4] showing that a stress-free crystal at 5 °K can be obtained by crossing the melting line at 3.8 kbar and 160 °K. A corresponding-states argument gives 4.5 kbar and 227 °K as the crossing point for krypton.

While the high-pressure technique offers distinct advantages in separating the volume and temperature dependences of the dispersion and additionally poses little difficulty as regards inelastic-neutron-scattering measurements, most *a priori* theoretical calculations and alternative experimental studies deal with an equilibrium crystal. Peter *et al.*[5] have measured the phonon dispersion for $0.04 < \vec{q} < 0.4$ Å^{-1} in an equilibrium crystal of krypton at 77 °K where $a = 5.744 \pm 0.005$ Å. These accurate resolution-corrected data enabled a precise determination of zero-sound elastic constants.

Similar motivation in determining zero-sound elastic constants was entailed in a small-$\vec{q}$ dispersion determination in an equilibrium krypton crystal at 114 °K by Skalyo and Endoh.[6] Here, near the triple point, an accurate comparison with first-sound elastic constants subsequently determined by Jackson *et al.*[7] using Brillouin scattering showed the first-sound elastic constants to be ~10% lower. The work presented here is a further study on an equilibrium crystal at 10 °K where a comparison is made with the theoretical dispersion curves calculated by Barker *et al.*[8] using an accurate two-body potential and a three-body force of the Axilrod-Teller type.[9] The result will also be

characterized by means of a Born–von Kármán force-constant analysis which will facilitate calculations of elastic constants, frequency distribution, and Debye temperatures characteristic of both the heat capacity and the Debye-Waller factor.

II. SAMPLES AND METHOD

The present crystal sample was grown at atmospheric pressure in the manner of Peterson *et al.*[10] The method has been used by Batchelder *et al.*[11] in a neutron investigation of solid argon and is such that a crystal is grown and measured *in situ*. Growth was in a Kapton[12] (polypyromelitimide) tube 9-mm-i.d. by 20-mm high and the apparatus is shown in Fig. 1. The tube was formed from Kapton film 0.05 mm thick and had a tapered overlapping glue joint[13] $1\frac{1}{2}$ mm wide. It was glued to an aluminum pedestal which was contained in an isothermal chamber connected to the copper block base of a variable-temperature cryostat. The top of the cell was a cap of stainless steel into which

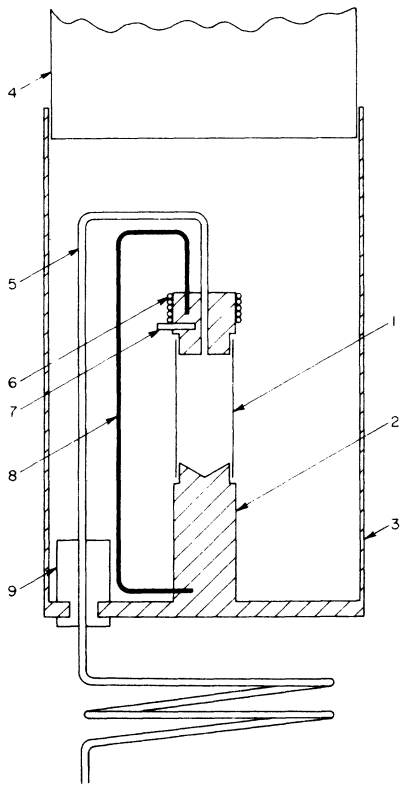

FIG. 1. Crystal growing cell: (1) Kapton tube; (2) aluminum base; (3) aluminum thermal shield; (4) temperature-controlled copper block; (5) stainless-steel tubing for supplying gas; (6) heater; (7) platinum resistance thermometer; (8) copper-wire thermal short, (9) thermally insulating nylon feedthrough.

was brazed the stainless-steel tubing ($1\frac{1}{2}$-mm-o.d. $\times$1-mm-i.d.) that supplied the research-grade krypton gas.[14] The top was thermally shorted to the base by $\approx$10 cm of copper wire 1 mm in diameter; this thermal short was easily circumvented by a 150-Ω heater wound on the cap.

The cell was initially allowed to fill with liquid and then the heater on the cap was adjusted to give a 3.5 °K higher temperature than the base of the cell. Platinum thermometers sensed the temperatures of the cap and base; two ac bridges sensed the balance points and controlled heaters, which kept the temperatures to within ±0.003 °K of the set point. The temperature settings were made on two ten-turn potentiometers which were mechanically geared to a synchronous timing motor that allowed a cooling of $\frac{1}{3}$ °K over an 8-h period; annealing at fixed temperature occurred for the next 16 h.

Upon complete solidification, the temperature differential was reduced and temperature control was provided by the base thermometer and heater alone. A neutron Polaroid picture of the (200) reflection at 114 °K showed the cell to be 95–100% one single crystal, and a rocking curve indicated a full width at half-maximum (FWHM) for the mosaic spread of less than 5 min. The zero-sound elastic constants[6] were measured at 114 °K as well as some neutron responses at the [100] zone boundary. Initially, it was our intention to free the crystal from the sample-cell wall before lowering the temperature by reducing the cell pressure below the equilibrium vapor pressure. This was negated by a blockage in the stainless-steel tubing and an alternative approach was used whereby the temperature was reduced at a continuous rate of 1 °K/day until 98 °K was reached. A change in the cooling to 3 °K/day then resulted in the first visible crack in the crystal; the mosaic spread was subsequently found to be 18 min at 84 °K. Cooling proceeded to 40 °K at which point the temperature was brought to 10 °K within 6 h, resulting in a final mosaic spread of 28 min; the lattice spacing was 5.646 ±0.002 Å.

The crystal grew with its [329] axis vertical, thus permitting scattering zones of [001] and [112] to be obtained with tilts of 21° and 14°, respectively. The measurements were performed on a triple-axis spectrometer at the Brookhaven High-Flux Beam reactor. A cylindrically curved monochromator and a flat analyzer[15,16] of pyrolytic graphite (002) were used with initial neutron energies E_i fixed at 13.5 or 14.5 meV; some [110] longitudinal modes near the zone boundary were measured with $E_i = 17.0$ meV. A pyrolytic graphite filter was used to eliminate higher-order contamination.[17,18] All collimators were 40 min, in order to obtain sufficient scattering intensities, except at the lowest

energies, where some 20-min collimators were used.

III. DISPERSION AT 10°K

Typical phonon scans are shown in Fig. 2. All phonon scans were fitted by the method of nonlinear least squares to Gaussians giving the peak positions and widths; the latter were due solely to instrumental resolution. The peak positions are further corrected for resolution effects[3,5,6] utilizing a program by Werner and Pynn,[19] and the results are listed in Table I for all symmetry directions measured and are depicted in Fig. 3 along with the theoretical calculations of Barker *et al.*[8] Note is made of the lack of measurements for $\zeta < 0.1$; this is a direct consequence of the 28 min mosaic spread of the sample. Here, ζ is the reduced wave vector of the phonon, $\vec{\zeta}a^* = \vec{q}$. Many of the phonons were measured several times and in some instances measurements were made in each of the two scattering zones obtained. Appropriate averages are given in those instances.

By far, the most usual representation of the data is through the determination of the harmonic Born-von Kármán force constants.[20] The multitude of data is here reduced to a few parameters. The data have been analyzed by a program written by Svensson *et al.*,[21] where the minimized function was

$$\chi^2 = \frac{1}{N-P} \sum_{i=1}^{N} \left(\frac{\epsilon_{i0}^2 - \epsilon_{ic}^2}{2\sigma_i \epsilon_{i0}} \right)^2 , \tag{1}$$

where ϵ_{i0} and σ_i are the measured energy of the phonon and its standard deviation determined by the least-squares calculation, respectively, and P is the number of fitted parameters. Both the general tensor force model and the axially symmetric model were fitted to the data; the latter is a central-force model where each neighbor gives two parameters that relate to the first and second derivatives of the two-body potential as discussed by Lehman *et al.*[22]

TABLE I. Krypton 10 °K phonon energies.

ζ	[100]T	[100]L	[1$\bar{1}$0]T_1	[110]T_2	[110]L
0.10	···	···	···	···	1.47 ± 0.07
0.12	···	···	0.80 ± 0.05	···	···
0.15	1.01 ± 0.05	···	0.93 ± 0.03	···	2.21 ± 0.05
0.20	1.34 ± 0.05	1.91 ± 0.05	1.21 ± 0.03	1.90 ± 0.03	2.90 ± 0.05
0.25	1.65 ± 0.03	2.37 ± 0.07	1.52 ± 0.03	···	3.53 ± 0.07
0.30	1.99 ± 0.03	2.79 ± 0.05	1.82 ± 0.03	2.78 ± 0.03	4.04 ± 0.03
0.35	2.30 ± 0.03	3.28 ± 0.03	2.12 ± 0.03	3.18 ± 0.03	4.50 ± 0.03
0.40	2.56 ± 0.03	3.58 ± 0.03	2.39 ± 0.03	3.61 ± 0.03	4.87 ± 0.05
0.445	···	···	···	···	5.16 ± 0.05
0.45	2.83 ± 0.03	4.01 ± 0.05	2.66 ± 0.03	3.98 ± 0.05	···
0.50	3.09 ± 0.03	4.34 ± 0.05	2.94 ± 0.03	4.36 ± 0.05	5.41 ± 0.05
0.55	3.32 ± 0.03	···	3.17 ± 0.03	4.65 ± 0.07	5.48 ± 0.05
0.60	3.53 ± 0.03	4.98 ± 0.05	3.36 ± 0.03	4.99 ± 0.07	5.49 ± 0.05
0.65	3.71 ± 0.03	···	3.58 ± 0.03	···	5.41 ± 0.05
0.70	3.87 ± 0.03	5.52 ± 0.05	3.75 ± 0.03	···	5.33 ± 0.05
0.75	···	···	3.93 ± 0.03	5.75 ± 0.05	5.13 ± 0.05
0.80	4.15 ± 0.05	···	4.04 ± 0.03	···	4.96 ± 0.05
0.85	···	6.02 ± 0.05	4.18 ± 0.03	···	4.75 ± 0.05
0.90	4.26 ± 0.05	···	4.29 ± 0.03	6.00 ± 0.10	4.58 ± 0.03
0.95	···	···	4.30 ± 0.03	···	4.44 ± 0.03
1.00	4.34 ± 0.05	6.20 ± 0.07	···	···	···

ζ	[111]T	[1$\bar{1}$1]L	Λ	Π
0.08	···	1.52 ± 0.05	···	···
0.10	0.90 ± 0.03	1.84 ± 0.05	···	···
0.15	1.34 ± 0.03	2.80 ± 0.05	···	···
0.20	1.71 ± 0.03	3.57 ± 0.05	···	···
0.24	2.01 ± 0.03	···	···	···
0.25	2.08 ± 0.03	4.33 ± 0.05	4.33 ± 0.03	5.93 ± 0.07
0.30	2.38 ± 0.03	5.04 ± 0.05	···	···
0.35	2.58 ± 0.03	5.57 ± 0.07	···	···
0.40	2.78 ± 0.03	5.94 ± 0.07	···	···
0.45	2.88 ± 0.03	6.12 ± 0.05	···	···
0.50	2.94 ± 0.03	6.27 ± 0.05	4.28 ± 0.05	5.40 ± 0.07
0.75	*	*	···	4.62 ± 0.05
1.00	*	*	···	···

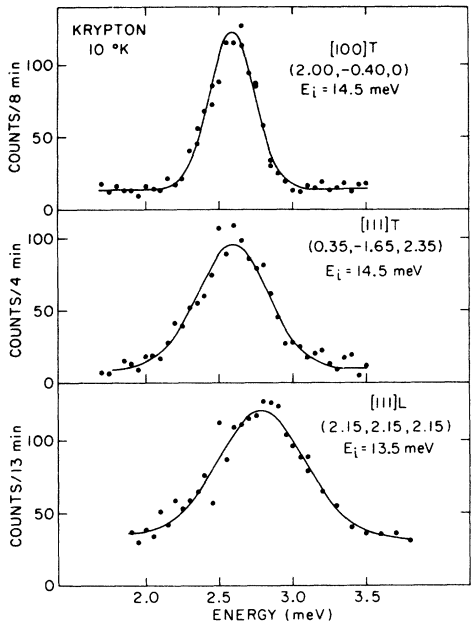

FIG. 2. Typical phonon scans of [100]T, [111]T, and [111]L modes at 10 °K.

TABLE II. Interatomic force constants in dyn cm^{-1}. Model 1 is an axially symmetric three-neighbor fit; model 2 is a general-force three-neighbor fit. Model 3 is an eight-neighbor fit where the first three neighbors are fit to general forces and the 4–8 neighbors are given by an axially symmetric force derived from the theoretical van der Waals potential of Ref. 24. [For general forces, symmetry requires $1YY = 1XX$, $1YZ = 1XZ = 0$, $2ZZ = 2YY$, $2YZ = 2XZ = 2XY = 0$, $3ZZ = 3YY$, and $3XY = 3XZ$. For axially symmetric forces, one has additionally $\alpha = 1XX - 1ZZ - 1XY$, $\beta = 3XX - 3YY - 3(3YZ)$, $\gamma = 2(3XX) - 2(3YY) - 3(3XZ)$ where $\alpha = \beta = \gamma = 0$.]

Force constant	Model 1	Model 2	Model 3
$1XX$	784 ± 4	773 ± 6	774 ± 6
$1ZZ$	−29 ± 3	−12 ± 6	−15 ± 6
$1XY$	813 ± 5	818 ± 6	820 ± 6
$2XX$	−42 ± 5	−22 ± 8	−19 ± 9
$2YY$	−4 ± 4	−8 ± 6	−8 ± 6
$3XX$	−2 ± 2	−5 ± 3	−3 ± 3
$3YY$	1 ± 1	2 ± 2	3 ± 2
$3YZ$	−1 ± 1	4 ± 2	3 ± 2
$3XZ$	−2 ± 1	−4 ± 1	−4 ± 1
α	0	−32 ± 13	−31 ± 13
β	0	−18 ± 9	−16 ± 9
γ	0	−1 ± 9	−1 ± 9

The results of the force-constant fits are given in Table II. For both models, the statistical F test finds that the fourth neighbor does not significantly improve the fit; i.e., for further neighbors, the force constants are smaller than their standard deviations which are ≈ 5 dyn cm^{-1}. We note that the deviation from the axially symmetric conditions as given by α, β, and γ in Table II are about twice the standard deviations for α and β. We believe this shows that a small but significant departure from the axially symmetric conditions is found in krypton, in contradistinction to neon where no significant deviations from the axially symmetric conditions were found.[3]

It is not to be implied that the far neighbors supply zero force, but to indicate that the accuracy of the present phonon measurements is insufficient for their determination. We have therefore made a fit to a general force-constant model for the first three neighbors, and additionally utilized a theoretical potential to calculate the axially symmetric forces for neighbors 4–8.[23] The van der Waals po-

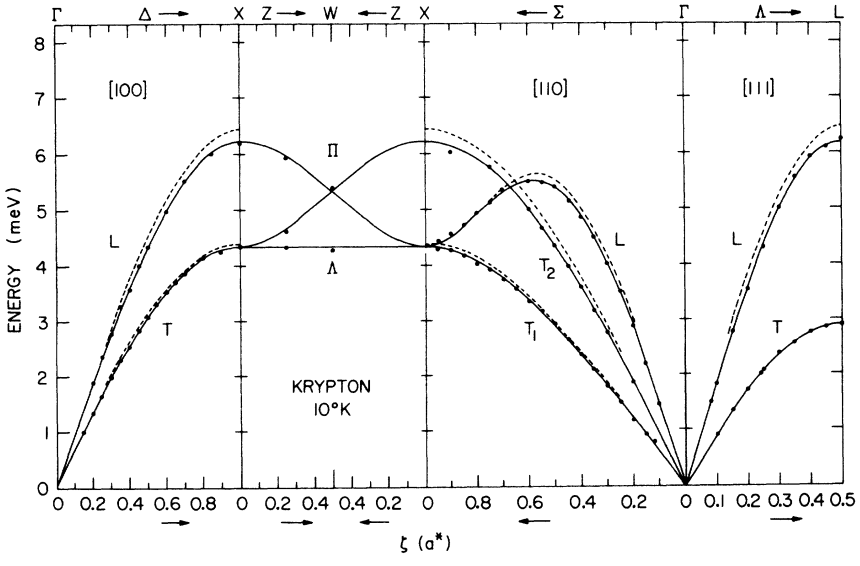

FIG. 3. Phonon dispersion of krypton at 10 °K. ζ is the reduced wave vector. The solid line is a three-nearest-neighbor general force-constant fit to the data and the dashed line is a theoretical calculation by Barker *et al.* (Ref. 8).

tential utilized was that derived by Starkschall and Gordon[24] where

$$\phi = -(1.245\times10^{-10}\ \text{erg Å}^6)/r^6$$

which is noted to be approximately half the strength one obtains when utilizing parameters for an appropriate Lennard-Jones 6–12 potential. The fit to the first three neighbors with the aforementioned condition is also included in Table II as model 3.

The limiting value of χ^2 defined by Eq. (1) was ≈ 6 for all models, which together with random errors indicated values of σ_i obtained by the least-squares fits to Gaussians were too low by a factor of ≈ 2.5. This was also similar to results obtained in the case of neon.[3] This factor has already been included in the phonon standard deviations given in Table I.

We have further utilized the derived force constants of model 3 to calculate the energy density of states $g(\nu)$ by the method of Gilat and Raubenheimer[25]; the result shown in Fig. 4 is a histogram based on a channel width of 0.001 THz and the number of mesh points in the irreducible zone was 75 614.

The moments M_n and associated Debye frequencies ν_n[26] of the frequency distribution have been calculated for $-3 < n \leq 30$ from

$$M_n = \int \nu^n g(\nu)\,d\nu\ , \qquad n > -3$$
$$\nu_n = [\tfrac{1}{3}(n+3)M_n]^{1/n}\ , \qquad n \neq 0 \text{ or } -3 \tag{3}$$
$$\nu_0 = \exp[\tfrac{1}{3} + \int g(\nu)\ln\nu\,d\nu]\ ,$$

and the results for ν_n are shown in Fig. 5. The various ν_n relate to characteristic Debye temperatures which for a Debye solid would give the same value to a certain thermodynamic property as calculated by using the actual frequency distributions; and for a solid with a Debye frequency distribution

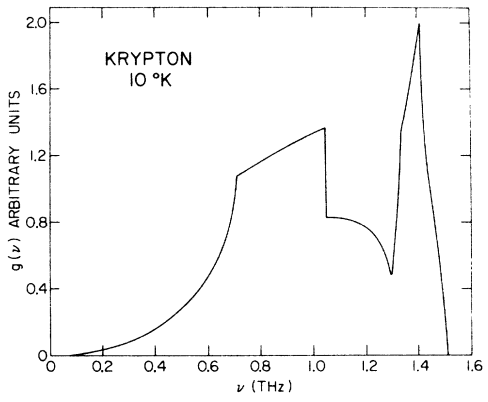

FIG. 4. Frequency distribution of krypton at 10 °K. The units are such that $\int_0^\infty g(\nu)d\nu = 1$.

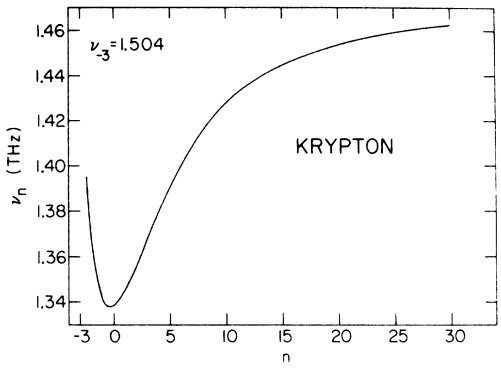

FIG. 5. Debye frequencies derived from the nth moment of the frequency distribution of Fig. 4.

$\nu_n = \nu_0$ for all n. For infinite and zero temperature, the Debye temperatures for the specific heat, Debye-Waller factor, and entropy are

$$\Theta_0^c = h\nu_{-3}/k_B\ , \quad \Theta_\infty^c = h\nu_2/k_B\ ,$$
$$\Theta_0^M = h\nu_{-1}/k_B\ , \quad \Theta_\infty^M = h\nu_{-2}/k_B\ , \tag{4}$$
$$\Theta_\infty^S = h\nu_0/k_B\ .$$

Note is made of the rapid variation in Fig. 5 near $n = -3$; this is indicative of strong departure from a quadratic frequency dependence for small ν.

The relations of Eq. (4) relate to limits of temperature; the association of a Debye temperature to a particular property as calculated from a real frequency distribution therefore gives a variation with temperature for the Debye temperature between these limits. The frequency distribution has therefore been used to calculate the heat capacity and the Debye-Waller factor as a function of temperature and the results have been related to a variation with temperature of Debye temperature as shown in Fig. 6. The different values of $\Theta_D(T)$ are due to the fact that each property is calculated

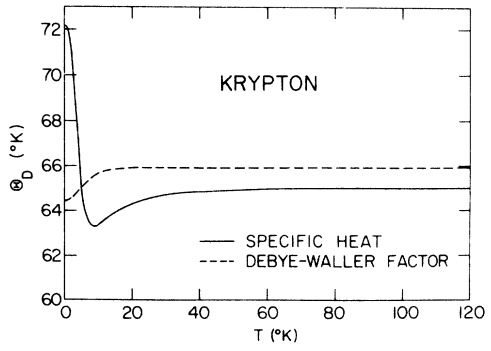

FIG. 6. Debye temperature variation for krypton at 10 °K, for the specific heat and for the Debye-Waller factor.

TABLE III. Elastic constants of krypton at 10 °K (in 10^8 dyn cm^{-2}). $B_0 = \frac{1}{3}(c_{11} + 2c_{12})$, $A = 2c_{44}/(c_{11} - c_{12})$, and $\delta = (c_{44} - c_{12})/c_{12}$. Models as described in Table II. The theoretical results are from Barker *et al.* (Ref. 8).

	Model 1	Model 2	Model 3	Theory
c_{11}	522 ± 5	521 ± 5	514 ± 5	506
c_{44}	268 ± 2	268 ± 3	268 ± 3	273
c_{12}	294 ± 7	292 ± 6	284 ± 6	287
B_0	370 ± 6	368 ± 5	361 ± 5	360
A	2.35 ± 0.05	2.34 ± 0.05	2.33 ± 0.05	2.49
δ	−0.09 ± 0.02	−0.08 ± 0.02	−0.05 ± 0.02	−0.05

as a differently weighted sum over the frequency distribution. There is almost no variation for Θ_D^M while Θ_D^c varies quite rapidly near $T = 0$. Indeed the calculation here has been used to infer the value of ν_{-3} given in Fig. 5. Specific-heat measurements by Beaumont *et al.*[27] give Θ_D in agreement with Fig. 6 to within 1% for $T < 20$ °K; the difference increases to 2% at 30 °K, with larger deviations above 30 °K due in part to the uncertainty of correcting C_p data to Θ_D related to the 0 °K volume.

An expansion of the low-frequency part of $g(\nu)$ is given in even powers of ν as

$$g(\nu) = a_2\nu^2 + a_4\nu^4 + a_6\nu^6 + \cdots \quad . \tag{5}$$

The calculated spectrum has been analyzed in the region $0 < \nu < 0.45$ THz for the first three coefficients, giving $a_2 = 0.882$ THz^{-2}, $a_4 = 0.75$ THz^{-4}, and $a_6 = 1.07$ THz^{-6}. The value for a_2 can also be obtained from the relation $a_2 = 3(\nu_{-3})^{-3}$.

Having made a representation of the data in terms of Born–von Kármán force constants, an extrapolation of the dispersion slopes as $\vec{q} \to 0$ can be utilized to obtain the zero-sound elastic constants. At $T = 0$ the difference between zero- and first-sound velocities is zero; one expects that the difference at 10 °K is within the errors and hence is of no consequence. The results of extrapolations for the three models of Table II are shown in Table III. The zero-sound bulk modulus $B_0 = \frac{1}{3}(c_{11} + 2c_{12})$, a measure of the anisotropy $A = 2c_{44}/(c_{11} - c_{12})$, and a measure of the deviation from the Cauchy relation $\delta = (c_{44} - c_{12})/c_{12}$ are also given.

The agreement between all models and the theory is quite good. The effect of the more distant neighbors as determined from Eq. (2) is seen to be small and possibly representative of the actual force. The results support the thesis that the three-body force introduced in the theory[8] is appropriate. Three-body effects have also been calculated by Hüller *et al.*[28] with a Lennard-Jones two-body potential giving $\delta = -0.07$; thus the heavy-krypton mass has reduced the sensitivity of δ to the form of the two-body potential. The values of $B_0 = (361 \pm 5) \times 10^8$ dyn cm^{-2} is higher than the x-ray value of Urvas *et al.*[29] of $(344 \pm 4) \times 10^8$ dyn cm^{-2} and the optical-interferometer value Coufal *et al.*[30] of $(341 \pm 3) \times 10^8$ dyn cm^{-2}; although at 10 °K we expect there should be a negligible difference. Finally, for completeness, we show in Fig. 7 the experimental neutron scattering results for the tem-

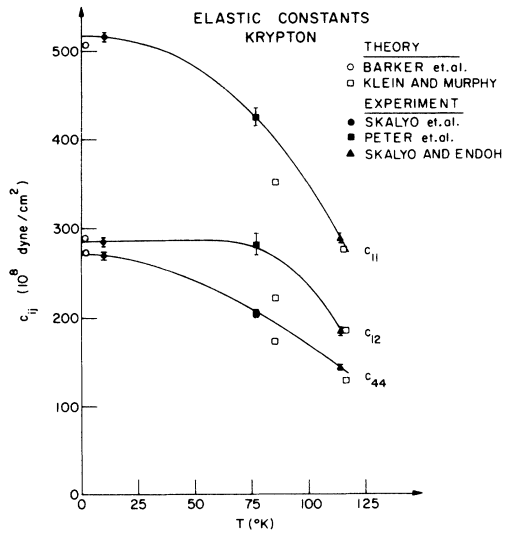

FIG. 7. Experimental neutron elastic constants and theoretical calculations vs temperature. The solid line is merely a guide.

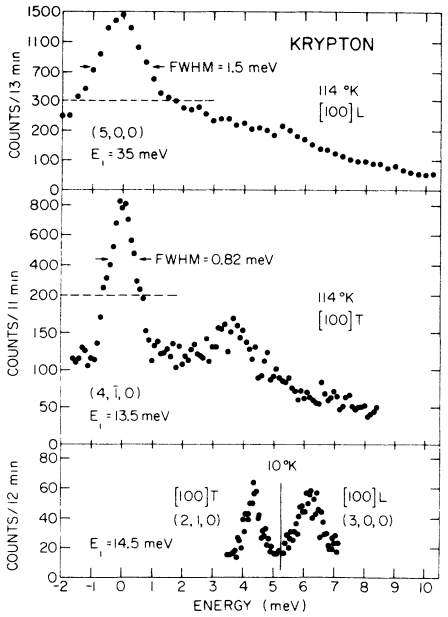

FIG. 8. The [100]L, T zone-boundary neutron response of krypton at 114 and 10 °K. Different instrumental resolutions have been used but do not substantially affect 114 °K data. Note the 10 °K data are a composite plot of two scans taken at two different reciprocal lattice positions.

perature variation of the elastic constants along with the theoretical calculations.

IV. PHONON LINEWIDTHS

Measurements were made of the neutron response at 114 °K (mp = 116 °K), where anharmonic effects on the single-phonon response are expected to be most pronounced. Complicating the observation, however, is an increased visibility of the multiphonon response, a consequence of which is evidenced in an increased Debye-Waller factor. An extensive study has not been attempted owing to the small sample size of ≈ 1.2 cm^3, small coherent cross section, and sample absorption.

Observed widths due only to an instrumental resolution of ≈ 0.1 meV were noted for $|\vec{q}| \lesssim 0.1$ Å^{-1}. Intrinsic broadening of ≈ 0.1 meV was observed for $|\vec{q}| \approx 0.15$ Å^{-1}, although with a small confidence level; a width of ≈ 0.8 meV and a peak at ≈ 1.9 meV were observed for a [100]T mode measured at (4, 0.4, 0) indicating a rapid increase in width between 0.15 and 0.60 Å^{-1}. Finally, at the zone boundary in the [100] direction the response has broadened substantially and is shown at the top of Fig. 8 for both the longitudinal and transverse modes. A separation of the response into components due to single-phonon and multiphonon scattering must await further studies with a larger crystal. The bottom of Fig. 8 contains the response measured at 10 °K for comparison; here, the widths are due to instrumental resolution alone.

The nature of the [100]T, L zone-boundary responses near $E = 0$ are obscured by an incoherent elastic scattering peak which has a width as indicated that is due to instrumental resolution. A subtraction of the incoherent scattering cannot be made from the present data, and it is therefore difficult to say whether the [100]L scan has a maximum at finite energy; the [100]T scan does peak near 3.5 meV, but this is a peak in the total response and not necessarily the single-phonon peak. The scan of the lower part of Fig. 8 are those of the weakest scattering intensities observed; a consequence of the term $[n(E)+1]/E$ in the scattering cross section. These scans should be compared with those shown in Fig. 2.

ACKNOWLEDGMENTS

The authors thank F. Langdon, W. Lenz, F. Thomsen, and P. Pyne for aid in the design and construction of the crystal-growing apparatus. We are much indebted to D. Batchelder and H. Peter for discussions relating to crystal growing and to M. L. Klein for discussions of interatomic potentials.

---

*Work performed under the auspices of the U. S. Atomic Energy Commission.

†On leave from Tohoku University, Sendai, Japan.

[1]W. B. Daniels, G. Shirane, B. C. Frazer, H. Umebayashi, and J. A. Leake, Phys. Rev. Lett. 18, 548 (1967).

[2]J. A. Leake, W. B. Daniels, J. Skalyo, Jr., B. C. Frazer, and G. Shirane, Phys. Rev. 181, 1251 (1969).

[3]J. Skalyo, Jr., V. J. Minkiewicz, G. Shirane, and W. B. Daniels, Phys. Rev. B 6, 4766 (1972).

[4]R. K. Crawford and W. B. Daniels, Phys. Rev. Lett. 21, 367 (1968).

[5]H. Peter, J. Skalyo, Jr., H. Grimm, E. Lüscher, and P. Korpiun, J. Phys. Chem. Solids 34, 255 (1973).

[6]J. Skalyo, Jr. and Y. Endoh, Phys. Rev. B 7, 4670 (1973).

[7]H. E. Jackson, D. Landheer, and B. P. Stoicheff, Phys. Rev. Lett. 31, 296 (1973).

[8]J. A. Barker, M. V. Bobetic, and M. L. Klein, Phys. Lett. A 34, 415 (1971).

[9]J. A. Barker, M. L. Klein, and M. V. Bobetic, Phys. Rev. B 2, 4176 (1970).

[10]O. G. Peterson, D. N. Batchelder, and R. O. Simmons, J. Appl. Phys. 36, 2682 (1965).

[11]D. N. Batchelder, M. F. Collins, B. C. G. Haywood, and G. R. Sidey, J. Phys. C 3, 249 (1970).

[12]E. I. Du Pont De Nemours & Co., Film Department, East Orange, N. J.

[13]Scotchcast electrical resin No. 8, 3M Company, St. Paul, Minn.

[14]Airco Industrial Gases, Murray Hill, N. J.; stated purity > 99.995%.

[15]T. Riste, Nucl. Instrum. Methods 86, 1 (1970).

[16]A. C. Nunes and G. Shirane, Nucl. Instrum. Methods 95, 445 (1971).

[17]G. Shirane and V. J. Minkiewicz, Nucl. Instrum. Methods 89, 109 (1970).

[18]S. M. Shapiro and N. J. Chesser, Nucl. Instrum. Methods 101, 183 (1972).

[19]S. A. Werner and R. Pynn, J. Appl. Phys. 42, 4736 (1971); also R. Pynn and S. A. Werner, Studsvik, Sweden, Laboratory Report No. AE-FF-112-Rev.

[20]B. N. Brockhouse, E. D. Hallman, and S. C. Ng, in *Magnetic and Inelastic Scattering of Neutrons by Metals*, edited by T. J. Rowland and P. A. Beck (Gordon and Breach, New York, 1968).

[21]E. C. Svensson, B. N. Brockhouse, and J. M. Rowe, Phys. Rev. 155, 619 (1967).

[22]G. W. Lehman, T. Wolfram, and R. E. deWames, Phys. Rev. 128, 1593 (1962).

[23]This procedure was suggested to us by W. B. Daniels, and M. L. Klein has suggested the potential utilized.

[24]G. Starkschall and R. G. Gordon, J. Chem. Phys. 54, 663 (1971).

[25]G. Gilat and L. J. Raubenheimer, Phys. Rev. 144, 390 (1966).

[26]T. H. K. Barron, W. T. Berg, and J. A. Morrison, Proc. R. Soc. A 242, 478 (1957).

[27]R. H. Beaumont, H. Chihara, and J. A. Morrison, Proc. Phys. Soc. (Lond.) 78, 1462 (1961).

[28]A. Hüller, W. Götze, and H. Schmidt, Z. Phys. 231, 173 (1970).

[29]R. O. Urvas, D. L. Losee, and R. O. Simmons, J. Phys. Chem. Solids 28, 2269 (1967).

[30]J. J. Coufal, R. Veith, P. Korpiun, and E. Lüscher, J. Appl. Phys. 41, 5082 (1970).